

# Three-dimensional subwavelength confinement of terahertz electromagnetic surface modes in a coupled slit structure

Jin-Kyu Yang,<sup>1</sup> Chul-Sik Kee,<sup>2,3</sup> and Joong Wook Lee<sup>2\*</sup>

<sup>1</sup>Department of Optical Engineering, Kongju National University, Kongju, 314-701 Korea

<sup>2</sup>Nanophotonics Laboratory, Advanced Photonics Research Institute (APRI), GIST, Gwangju, 500-712, Korea

<sup>3</sup>Center for Subwavelength Optics, Korea

[leejuj@gist.ac.kr](mailto:leejuj@gist.ac.kr)

**Abstract:** We report on the three-dimensional subwavelength confinement of the electromagnetic waves at a coupled metallic slit structure beyond diffraction limit in terahertz region. Lateral confinement behavior, leading to the three-dimensional confinement, is caused by a strong funneling effect of the light which occurs at the intersection of slits with a sharp metal geometry. Tunability of the resonant frequency and the position of the light confinement is achieved by controlling the slit length and the position of the intersection of slits, respectively.

©2011 Optical Society of America

**OCIS codes:** (300.6495) Spectroscopy, Terahertz; (240.6680) Surface plasmons; (260.3910) Metal optics.

---

## References and links

1. W. L. Barnes, A. Dereux, and T. W. Ebbesen, "Surface plasmon subwavelength optics," *Nature* **424**(6950), 824–830 (2003).
2. C. Genet and T. W. Ebbesen, "Light in tiny holes," *Nature* **445**(7123), 39–46 (2007).
3. Y. Kawano and K. Ishibashi, "An on-chip near-field terahertz probe and detector," *Nat. Photonics* **2**(10), 618–621 (2008).
4. H. Yoshida, Y. Ogawa, Y. Kawai, S. Hayashi, A. Hayashi, C. Otani, E. Kato, F. Miyamaru, and K. Kawase, "Terahertz sensing method for protein detection using a thin metallic mesh," *Appl. Phys. Lett.* **91**(25), 253901 (2007).
5. C. M. Bingham, H. Tao, X. Liu, R. D. Averitt, X. Zhang, and W. J. Padilla, "Planar wallpaper group metamaterials for novel terahertz applications," *Opt. Express* **16**(23), 18565–18575 (2008).
6. J. B. Pendry, L. Martín-Moreno, and F. J. García-Vidal, "Mimicking surface plasmons with structured surfaces," *Science* **305**(5685), 847–848 (2004).
7. F. J. García-Vidal, L. Martín-Moreno, and J. B. Pendry, "Surfaces with holes in them: new plasmonic metamaterials," *J. Opt. A, Pure Appl. Opt.* **7**(2), S97–S101 (2005).
8. Y. Takakura, "Optical resonance in a narrow slit in a thick metallic screen," *Phys. Rev. Lett.* **86**(24), 5601–5603 (2001).
9. F. Yang and J. R. Sambles, "Resonant transmission of microwaves through a narrow metallic slit," *Phys. Rev. Lett.* **89**(6), 063901 (2002).
10. F. J. García-Vidal, E. Moreno, J. A. Porto, and L. Martín-Moreno, "Transmission of light through a single rectangular hole," *Phys. Rev. Lett.* **95**(10), 103901 (2005).
11. J. W. Lee, M. A. Seo, D. H. Kang, K. S. Khim, S. C. Jeoung, and D. S. Kim, "Terahertz electromagnetic wave transmission through random arrays of single rectangular holes and slits in thin metallic sheets," *Phys. Rev. Lett.* **99**(13), 137401 (2007).
12. J. W. Lee, M. A. Seo, D. J. Park, D. S. Kim, S. C. Jeoung, Ch. Lienau, Q. H. Park, and P. C. M. Planken, "Shape resonance omni-directional terahertz filters with near-unity transmittance," *Opt. Express* **14**(3), 1253–1259 (2006).
13. J. W. Lee, M. A. Seo, D. J. Park, S. C. Jeoung, Q. H. Park, Ch. Lienau, and D. S. Kim, "Terahertz transparency at Fabry-Perot resonances of periodic slit arrays in a metal plate: experiment and theory," *Opt. Express* **14**(26), 12637–12643 (2006).
14. M. A. Seo, H. R. Park, S. M. Koo, D. J. Park, J. H. Kang, O. K. Suwal, S. S. Choi, P. C. M. Planken, G. S. Park, N. K. Park, Q. H. Park, and D. S. Kim, "Terahertz field enhancement by a metallic nano slit operating beyond the skin-depth limit," *Nat. Photonics* **3**(3), 152–156 (2009).
15. A. Devilez, N. Bonod, J. Wenger, D. Gérard, B. Stout, H. Rigneault, and E. Popov, "Three-dimensional subwavelength confinement of light with dielectric microspheres," *Opt. Express* **17**(4), 2089–2094 (2009).

16. M. K. Seo, S. H. Kwon, H. S. Ee, and H. G. Park, "Full three-dimensional subwavelength high-Q surface-plasmon-polariton cavity," *Nano Lett.* **9**(12), 4078–4082 (2009).
  17. X. L. Zhu, Y. Ma, J. S. Zhang, J. Xu, X. F. Wu, Y. Zhang, X. B. Han, Q. Fu, Z. M. Liao, L. Chen, and D. P. Yu, "Confined three-dimensional plasmon modes inside a ring-shaped nanocavity on a silver film imaged by cathodoluminescence microscopy," *Phys. Rev. Lett.* **105**(12), 127402 (2010).
  18. L. Chen, J. Shakya, and M. Lipson, "Subwavelength confinement in an integrated metal slot waveguide on silicon," *Opt. Lett.* **31**(14), 2133–2135 (2006).
  19. H. Zhan, R. Mendis, and D. M. Mittleman, "Superfocusing terahertz waves below  $\lambda/250$  using plasmonic parallel-plate waveguides," *Opt. Express* **18**(9), 9643–9650 (2010).
  20. S. A. Maier, S. R. Andrews, L. Martín-Moreno, and F. J. García-Vidal, "Terahertz surface plasmon-polariton propagation and focusing on periodically corrugated metal wires," *Phys. Rev. Lett.* **97**(17), 176805 (2006).
- 

## 1. Introduction

Controlling light on scales much smaller than the wavelength has great potential for electronic, photonic, and biotechnology applications [1, 2]. Tight focusing of terahertz (THz) waves into subwavelength area has been especially important for applications based on highly sensitive bio-sensors with high resolution [3–5]. The excitations of guided modes supported by designer surface plasmons, which are confined surface modes observed on highly conducting surfaces perforated by subwavelength apertures, have arisen as a promising candidate for realizing strong confinement of the electromagnetic waves beyond the diffraction limit [6, 7]. The subwavelength confinement causes the electric field enhancement in one- (1-) and two-dimensional (2-D) apertures, even in the perfect-conductor regime [8–10]. There were several reports about the local field enhancement maximized by designing metallic structures consisted of high aspect-ratio rectangular holes or various shapes of apertures [11–13]. Recently, it was reported that an extremely narrow metallic nano slit shows a field enhancement of more than ten thousand times [14]. While these showed a 2-D subwavelength confinement mostly, there was no report about a three-dimensional (3-D) confinement with a high tunability in the resonant frequency and the position of the light confinement. Even in case of showing a 3-D confinement which appears in specific structures like a circular hole, the confinement efficiency was very low and the tunability in the resonant frequency and the position were not controllable. A new design of structured metals is therefore required to obtain the characteristics of the full 3-D subwavelength confinement and the tunability in the resonant frequency and the position of the light confinement. Even though there have been lots of efforts for realizing the strong confinement into a small area by using subwavelength cavities, dielectric microspheres, metallic tips, or etc [15–20], achieving the strong 3-D subwavelength confinement in the structured metals consisted of perforated apertures is still important, since those will be a basic component of plasmonic circuits or microfluidic devices which may be applied for sensing applications.

In this paper, we investigate an innovative technique for the 3-D subwavelength confinement of THz electromagnetic surface modes in a periodic arrangement of coupled slit structures crossed at a single position. The theoretical simulations based on the 3-D finite-difference time-domain (FDTD) method show that the resonant frequency of the surface mode is related with the fundamental mode of the single slit. The spatial distribution of the resonant electric field along the slab is determined by its structural shape, not the wavelength of the incident light, which enables the efficient 3-D electric field confinement beyond the diffraction limit. Our results support that the 3-D subwavelength confinement may result from carrier concentration on a narrow gap formed by overlapping three slits with different angles. We can also realize the tunability in the resonant frequency, while still achieving the strong near-field enhancement, without significantly changing their spatial resolution characteristics. Moreover, the position of the light confinement becomes controllable by changing the position of the intersection of slits.

## 2. Results and discussion

The coupled slit structure composed of three slits is perforated in a 25  $\mu\text{m}$ -thick aluminum film, as shown in Fig. 1(a). Here, two slits with oblique angles of 10 and  $-10$  degrees are overlapped on a single slit which is parallel to the y-axis. The length ( $l$ ) and the width ( $d$ ) of

all the slits are 600  $\mu\text{m}$  and 10  $\mu\text{m}$ , respectively. The coupled slit structures are arranged to form the square lattice with periods of  $\Delta x=400$   $\mu\text{m}$  and  $\Delta y=800$   $\mu\text{m}$  for an efficient implementation of the periodic boundary condition in the FDTD analysis. The structure is illuminated by normally incident THz radiation polarized parallel to the  $x$ -axis. Zero-order transmission spectra and near electric-field distributions of resonant surface plasmon modes are obtained by the numerical simulations. The results are compared with one obtained from a single slit in each unit.

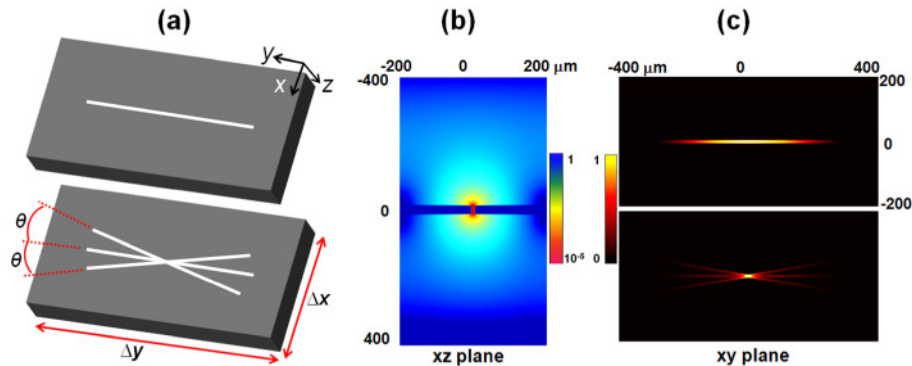


Fig. 1. (a) Schematic illustration of a single slit (upper) and a coupled slit structure (lower), in each unit.  $\Delta x$  and  $\Delta y$  are the  $x$ - and  $y$ -axis periods, respectively. (b) The  $xz$ -cut view of the electric field intensity distribution of the single slit in logarithmic scale at the resonant frequency of 0.22 THz. (c) The  $xy$ -cut view of the electric field intensity distribution ( $E_x^2 + E_y^2$ ) of the single slit structure (upper) and the coupled slit structure (lower) at the surface of metal film.

Figure 1(b) shows the  $xz$ -cut view of the electric field intensity distribution of the single slit structure at the resonant frequency of 0.22 THz (the resonant wavelength  $\lambda_R \sim 1.4$  mm). The electric field distribution shows strong subwavelength confinement and enhancement inside the slit because the thickness and the width of the single slit are much smaller than the incident THz wavelength. The degrees of field confinement along the  $x$  and  $z$  axes are roughly  $\lambda_R/(10 \mu\text{m})=140$  and  $\lambda_R/(25 \mu\text{m})=52$ , respectively, which are surprisingly high degrees compared with the so-called diffraction limit of light.

The electric field intensity distribution of the single slit structure in the  $xy$  plane [the upper figure in Fig. 1(c)], however, shows a wide distribution of the in-plane electric field over the slit aperture. For achieving the 3-D subwavelength confinement, the lateral field confinement along the  $y$  axis is required. The in-plane electric field profile of the coupled slit structure (the lower figure in Fig. 1(c)) shows the distinguishable confinement at the center of the slits. The coupled slit structure enables to confine the electric field in a 3-D subwavelength area simply by adding two oblique slits on the single slit. Here, the degree of lateral confinement along the  $y$  axis is determined by the structural shape at the intersection area of the three slits such as the slit width and the degree of angle between slits. The lateral confinement behavior is caused by a strong funneling effect of the light through the extremely narrow intersection area, and in turn leads to the 3-D confinement of the electric field. For the slit length of  $l=600$   $\mu\text{m}$ , the spatial resolution along the  $y$ -axis becomes at least ten times better than that in the simple slit structure.

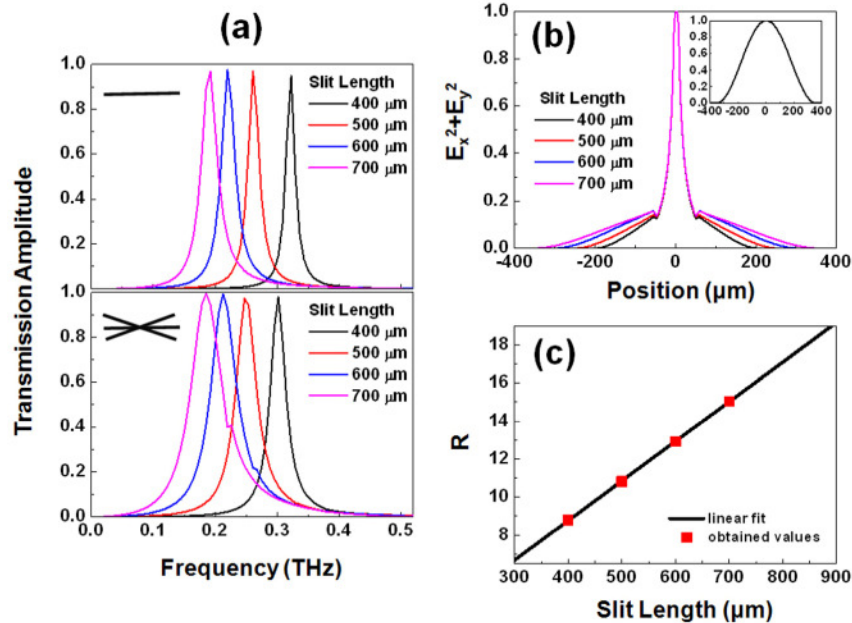


Fig. 2. (a) Transmission spectra through the single slit structures (upper) and the coupled slit structures (lower), at normal incident wave polarized perpendicular to the slit. The length of the slits are varied from 400  $\mu\text{m}$  to 700  $\mu\text{m}$  with a step of 100  $\mu\text{m}$ . (b) The electric field profiles along the slit, obtained in the plane of metal surfaces of the coupled slit structures. The inset shows a simulation of electric field obtained from the single slit structure with the length of 700  $\mu\text{m}$ . (c) The ratios between FWHM values of the electric field profile on a single slit structure ( $F_s$ ) and that on a coupled slit structure ( $F_t$ ). A black line was from the linear fitting of the ratios.

To quantitatively describe the degree of the lateral field confinement and to control resonant frequency, we studied the effect of varying the length of the slits on characteristics of the resonant surface mode. Note that the resonant frequency and the spatial resolution of the 3-D confinement region are related to the structural parameters of the slits. This means that the resonant wavelength can be tuned by varying the length of the slits, while the spatial resolution is maintained since the shape of the intersection area is still same despite of varying the length of the slits.

Figure 2(a) shows the amplitude transmission spectra of the single and coupled slit structures with different lengths. The transmission peaks are found near the frequencies of the fundamental resonant modes,  $f_R = c/2l$ . The resonances are broadened and shift to shorter frequencies as the slit length decreases because the slit has a finite width with a shallow depth and the coupled slit effectively acts as a wider slit in the far-field zone. Interestingly, the spatial profiles of the electric field intensity along the slits [Fig. 2(b)] look exactly the same, despite of different lengths of the slits. It implies that the degree of the 3-D subwavelength confinement is affected by the structural shape of the intersection area, not the length of the slits. Therefore, the resonant frequency is controlled by varying the length of the slits, without losing the spatial resolution and the confinement efficiency.

For the quantitative analysis of the confinement efficiency, the relation between the resonant frequency and the efficiency ratio was studied. The electric field distributions for the single slit structures as shown in the inset of Fig. 2(b) are changed as the slits have different lengths (not shown here). In contrast, the results for the coupled slit structures do not show any change in their spatial resolution. Here, we define the ratio of the full-width-half-maximum (FWHM) values obtained from the electric field distributions, as a confinement factor,  $R = F_s/F_t$ , where  $F_s$  and  $F_t$  are the FWHM values for the single slit structure and the coupled one, respectively. Figure 2(c) shows that the confinement factor is linearly

proportional to the length of the slits which determines the resonant frequency. From the results, it is possible to optimize the confinement factor by increasing the resonant frequency or by modifying the structural shape at the intersection area. The structures may actually act as a *frequency-controllable* single pore, which is currently receiving a great deal of attention for applications in biological sensing.

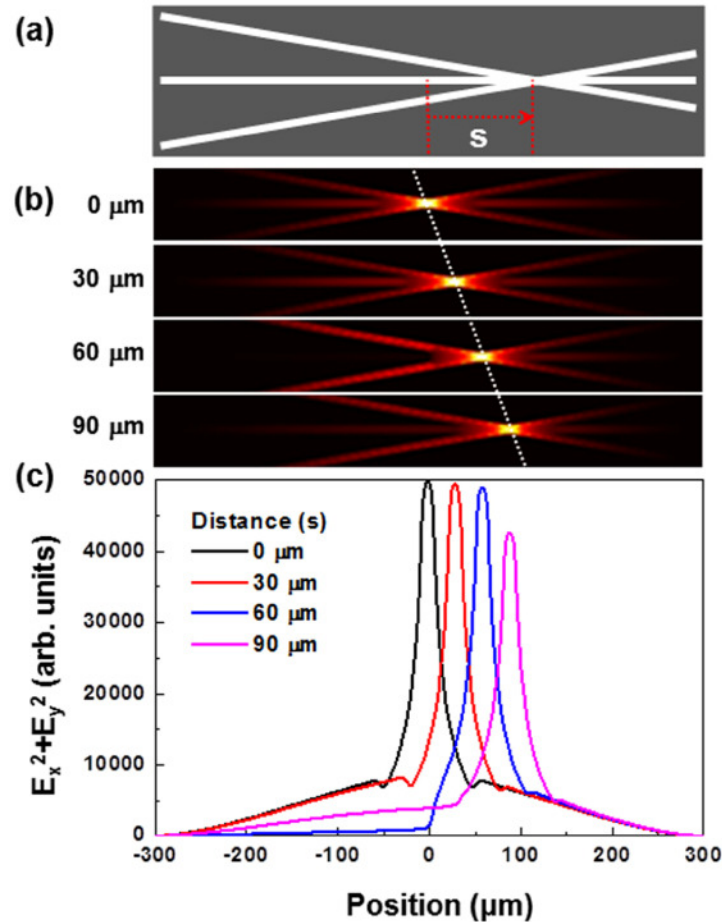


Fig. 3. (a) Schematic illustration of a coupled slit structure, which has an intersection position located on an off-center site. A distance from the center of each slit is defined as an off-center parameter,  $S$ .  $S$  is varied in the range from 0  $\mu\text{m}$  to 90  $\mu\text{m}$  with a step of 30  $\mu\text{m}$ , while the other structural parameters like the length and the shape of slits are kept constant. (b) The  $xy$ -cut view of the electric field intensity distribution ( $E_x^2 + E_y^2$ ) of a coupled slit structures with different off-center parameters of 0, 30, 60 and 90  $\mu\text{m}$ , at the surface of metal film. The electric intensity distributions are obtained at the resonant frequencies of each structure. (c) The electric field profiles along the center slit.

Another advantage of the coupled slit structures is that the spatial position of the electric field confinement can be tuned by shifting the intersection position. Figure 3(a) shows the schematic illustration of a coupled slit structure, which has an off-center parameter;  $S$ .  $S$  is varied in the range from 0  $\mu\text{m}$  to 90  $\mu\text{m}$  with a step of 30  $\mu\text{m}$ , while the other structural parameters like the length and the shape of slits are kept constant. Figure 3(b) shows the electric field distributions obtained in the surface of metal film. This reveals that the spatial position of the 3-D subwavelength confinement always found at the intersection area of slits, without any change of the FWHM value and the resonant frequency, which is clearly verified by the electric field profiles along the center slit as shown in Fig. 3(c). Interestingly, the spatial profiles show strong confinement of the resonant mode even at higher off-center parameters. The structures may be regarded as a *position-controllable* single pore.

### **3. Conclusion**

In conclusion, we have achieved the 3-D subwavelength confinement of THz electromagnetic waves with the coupled slit structure. The 3-D confinement is caused by the lateral confinement due to the strong funneling effect of the light through the intersection area of the slits with a sharp metal geometry. The tunability in the resonant frequency and the position of the confinement is realized by modifying the structural parameters of the slit length and the intersection position, respectively. The structure therefore acts as a frequency- and position-controllable single pore on a metal sheet, having the characteristic of the 3-D subwavelength confinement. This approach will be useful for improving sensing technologies for applications in biological and chemical sensing.

### **Acknowledgments**

This research was supported by Basic Science Research Program through the National Research Foundation of Korea (NRF) funded by the Ministry of Education, Science and Technology (2010-0021181; 2010-0001858; 2010-0025701) and by the APRI Research Program of GIST.